HHS Public Access

Author manuscript

Prog Biophys Mol Biol. Author manuscript; available in PMC 2021 August 01.

Published in final edited form as:

Prog Biophys Mol Biol. 2020 August ; 154: 71–79. doi:10.1016/j.pbiomolbio.2019.04.008.

Three-dimensional encapsulation of adult mouse cardiomyocytes in hydrogels with tunable stiffness

Claudia Crocini[1,2,*], **Cierra J. Walker**[2,3,*], **Kristi Anseth**[1,2,4], **Leslie A. Leinwand**[1,2,#]

[1]Department of Molecular Cellular and Developmental Biology, University of Colorado Boulder, CO 80309, USA

[2]BioFrontiers Institute, University of Colorado Boulder, CO 80303, USA

[3]Materials Science and Engineering Program, University of Colorado Boulder, CO 80303, USA

[4]Department of Chemical and Biological Engineering, University of Colorado Boulder, CO 80303, USA

Abstract

Numerous diseases, including those of the heart, are characterized by increased stiffness due to excessive deposition of extracellular matrix proteins. Cardiomyocytes continuously adapt their morphology and function to the mechanical changes of their microenvironment. Because traditional cell culture is conducted on substrates that are many orders of magnitude stiffer than any environment encountered by a cardiomyocyte in health or disease, alternate culture systems are necessary to model these processes *in vitro*. Here, we employ photo-clickable thiol-ene poly(ethylene glycol) (PEG) hydrogels for three-dimensional cell culture of adult mouse cardiomyocytes. PEG hydrogels serve as versatile biocompatible scaffolds, whose stiffness can be precisely tuned to mimic physiological and pathological microenvironments. Compared to traditional culture, adult cardiomyocytes encapsulated in PEG hydrogels exhibited longer survival and preserved sarcomeric and T-tubular architecture. Culture in PEG hydrogels of varying stiffnesses regulated the subcellular localization of the mechanosensitive transcription factor, YAP, in adult cardiomyocytes, indicating PEG hydrogels offer a versatile platform to study the role of mechanical cues in cardiomyocyte biology.

1. Introduction

Nearly all etiologies of heart disease involve pathological remodeling of cardiac tissue characterized by activated cardiac fibroblasts (myofibroblasts), (Travers et al., 2016) depositing excessive extracellular matrix (ECM), which increases tissue stiffness and reduces cardiac function. Cardiomyocytes respond to alterations of ECM composition and stiffness by remodeling contractile properties and morphology, ultimately leading to

[#]correspondence to leslie.leinwand@colorado.edu.
[*]These authors contributed equally

maladaptive tissue remodeling (Gourdie et al., 2016; Kong et al., 2014; Porter and Turner, 2009). Mechanisms of mechanotransduction in cardiac myocytes have primarily been investigated in two dimensional cultures of neonatal cardiomyocytes and embryonic or induced pluripotent stem-cell derived cardiomyocytes (Chopra et al., 2012; Hazeltine et al., 2012; Ribeiro et al., 2015). These cellular models are inherently different than adult cardiomyocytes, limiting our understanding of mechanical signaling in adult cardiac tissue. The use of adult cardiomyocytes is further compromised by the deterioration of cellular integrity after only 1-2 days in culture. Arguably, the first hallmark associated with deterioration of cardiomyocytes in culture is the loss and remodeling of T-tubules (Banyasz et al., 2008; Lipp et al., 1996; Mitcheson et al., 1996). These are membrane invaginations responsible for action potential propagation (Brette and Orchard, 2003; Ferrantini et al., 2013). This gross alteration of cardiac cellular membranes limits *in vitro* work with adult cardiomyocytes. To date, the role of substrate stiffness in adult cardiomyocytes has been investigated with a two-dimensional (2D) culture system (Galie et al., 2013). However, 2D cultures do not provide mechanical cues to the entirety of the cell, likely producing a blunted or non-physiologic cellular response to the environment. Conversely, three-dimensional (3D) culture systems could allow for improved presentation of mechanical cues. Commonly, 3D systems are used to develop engineered tissues using neonatal cardiomyocytes and embryonic or induced pluripotent stem-cell derived cardiomyocytes. These approaches have yielded remarkable maturity of cardiomyocytes (Hirt et al., 2014; Ronaldson-Bouchard et al., 2018; Ruan et al., 2016), but have not been used in adult cardiac myocytes.

Advances in synthetic biomaterial substrates have allowed the creation of synthetic ECM for spatial and temporal control over mechanical and biochemical cues (Leijten et al., 2017; Lin and Anseth, 2009). Due to their high water content, hydrogels can emulate the physical properties of soft tissues, and have been proven to be highly biocompatible for uses including tissue engineering and drug delivery (Tibbitt and Anseth, 2009). In particular, poly(ethylene glycol) (PEG) hydrogels are the most widely studied and applied (Zustiak and Leach, 2010). PEG cell culture systems have been developed where the mechanical microenvironment is highly controlled through crosslinking density of the polymer network. Specifically, thiol-ene click chemistry-based hydrogels offer fast and reliable polymerization and by using a photo-initiator, hydrogels can form cell-laden matrices with user-defined control of gel formation and the final material properties. This chemistry has proven extremely valuable for probing how cells respond and interact with their microenvironment (Rodriguez et al., 2018; Schultz et al., 2015).

Here, we generated a 3D culture system for single isolated cardiomyocytes employing PEG hydrogels, whose stiffness was finely modulated *in situ.* Isolated adult mouse ventricular cardiomyocytes (AMVMs) were encapsulated in PEG hydrogels of different stiffnesses. We found that sarcomeric and T-tubular architecture of cultured cardiomyocytes in PEG hydrogels is preserved. We demonstrated that functional measurements of single AMVMs in 3D are possible. Further, we found that the functional and molecular outputs of AMVMs are dependent on the PEG hydrogel stiffness. Our work highlights the use of 3D microenvironments to study the role of the mechanical signaling in cardiac biology and pathologies.

2. Material and Methods

Synthesis of poly(ethylene glycol)-norbornene (PEGnb)

8-arm PEGnb was synthesized as described previously (Benton et al., 2009; Fairbanks et al., 2009b). Briefly, stoichiometric amounts of 8-arm PEG (40, 20, or 10 kDa, JenKem) and 4-dimethylaminopyridine (Sigma Aldrich) were dissolved in anhydrous dichloromethane (Sigma Aldrich). A two-fold excess of each 5-norbornene-2-carboxylic acid (Sigma Aldrich) and N-N'-diisopropylcarbodiimide (Sigma Aldrich) were added and reaction vessel was purged with argon. After reacting overnight on ice while stirring, product was precipitated in 4°C ethyl ether (Fisher Scientific). The product was then filtered and dried by vacuum. Next, the PEGnb was dissolved in water and purified by dialysis. The final product was lyophilized, and the overall end group functionality was characterized by proton nuclear magnetic resonance imaging to confirm >90% functionalization.

Hydrogel fabrication

For soft hydrogels, 5 wt% 8-arm 40k PEGnb was crosslinked with 2 mM di-thiol PEG 5k and with 1 mM CRGDS (American Peptide Company, Inc), an adhesive peptide, at a ratio of 0.5 thiols per norbornene. For medium hydrogels, 5 wt% 8-arm 40k PEGnb was crosslinked with 4.5 mM di-thiol PEG 5k and with 1 mM CRGDS adhesive peptide (American Peptide Company, Inc) at a ratio of 1 thiol per norbornene. For stiff hydrogels, 5 wt% 8-arm 20k PEGnb was crosslinked with 1.125 mM 8-arm PEG thiol 10k and with 1 mM CRGDS adhesive peptide (American Peptide Company, Inc) at a ratio of 0.5 thiols per norbornene. The photoinitiator lithium phenyl-2,4,6-trimethylbenzoylphosphinate (LAP) was added at a concentration of 2.5 mM. All components were dissolved in phosphate buffered saline (PBS, Life Technologies). A shear rheometer (ARES; TA) was used to measure the modulus of the hydrogels. For rheology, hydrogels (thickness=150μm) were polymerized *in situ* between an 8-mm diameter tool. The hydrogels were polymerized by exposure to UV light (~2 mW/cm2 at 365 nm) for 90 seconds (Omnicure 1000, Lumen Dynamics). Network evolution was tracked using a dynamic time sweep (γ=1%; ω=1 rad/s; determined to be in the linear regime for this material) until the storage modulus (G') reached a plateau.

Tissue Rheology

The modulus of mouse left ventricles were measured with shear rheology. Hearts were excised from 6-8 week old mice, whereby an 8mm punch was used to cut out a cylindrical portion of the tissue. Left ventricle tissue was measured within 2 hours of isolation. Tissue was trimmed to ensure level/even height of <1 mm. A shear rheometer (ARES; TA) was used to measure the modulus of the left ventricle tissue, and sand paper was used between the parallel plate geometry to prevent tissue slippage.

Dynamic hydrogel stiffening

Hydrogels were stiffened as previously described (Mabry et al., 2015). Stiffening solutions were comprised of 8-arm 10 kDa PEG-norbornene (10 mM), 8-arm 10 kDa PEG-thiol (10 mM), and LAP (2.5 mM). Gels were soaked in the stiffening solution for 15 min. For non-stiffened hydrogels, the hydrogels were soaked in PBS (Sigma Aldrich) to create mock

stiffening treatment. Gels were then removed from solution and the excess swelling solution was blotted from the surface before polymerization with UV light (2 mW/cm2 at 365 nm) for 90 seconds. The shear modulus after stiffening was measured with a shear rheometer (ARES; TA) using swollen hydrogels. As with *in situ* rheology, both frequency sweeps and strain sweeps were performed to ensure that measurements were representative of the linear viscoelastic regime. The shear modulus (G0) was measured and converted to Young's modulus with 0.5 Poisson's ratio.

Adult mouse ventricular myocytes (AMVMs)

AMVMs were isolated from the left ventricle of 6-week old male mice using a retrograde Langendorff's perfusion system and enzymatic digestion (0.1 mg/ml Liberase TM, Sigma-Aldrich), as previously described (Crocini et al., 2016). Briefly, perfusion buffer solution contained (in mM): 113 NaCl, 14.7 KCl, 0.6 KH_2PO_4, 0.6 Na_2HPO_4, 1.2 $MgSO_4$-$7H_2O$, 12 $NaHCO_3$, 10 $KHCO_3$, 10 Hepes, 30 taurine, 10 glucose, 10 2,3-butanedione monoxime, pH 7.3 (adjusted with NaOH). Cells were gradually readapted to calcium in perfusion buffer added with 1% bovine serum albumin (BSA) by adding 50 or 100 μM $CaCl_2$ every 5-8 min, until a concentration of 500 μM $CaCl_2$ was reached.

3D encapsulation and culture of cardiomyocytes

Isolated AMVMs were resuspended in Minimum Essential Medium (MEM) α supplemented with 1 μg/ml Insulin, 0.55 μg/ml transferrin, 0.5 ng/ml selenium, 2 mM Glutamine, 10 mM NaHCO3, 10 mM HEPES, 0.2% Bovine serum albumin, and 25 μM blebbistatin. pH adjusted to 7.4 with NaOH (Louch et al., 2011). For 3D encapsulation, cardiac myocytes were used within one hour post-isolation and approximately 10^4 cells/ml were suspended in the monomer solution, and 30 μ of the cell-monomer solution were added to a mold (5 mm diameter, 1 mm height) placed on glass coverslip thiolated by vapor deposition of 3-(mercaptopropyl)trimethoxy-silane in an 80°C oven to facilitate covalent anchoring of the gels to the coverslips. Cells were allowed to settle by gravity for 2 minutes in the monomer solution, after which the hydrogels were polymerized by exposure to UV light (~2 mW/cm^2 at 365 nm) for 90 seconds. For extended culture, hydrogels were placed in blebbistatin-containing AMVM culture medium. For functional contraction, hydrogels were placed in tyrode buffer (see below). 2D cultures onto 20 μg/ml laminin-coated glass coverslips were used as control. AMVMs were incubated for 2 hours at 37°C 5% CO_2 to allow attachment to coverslips. 3D encapsulated AMVMs were incubated likewise before other experiments. Culture medium was changed every other day.

Cell viability analysis

Cell viability was measured using a Live/Dead cytotoxicity kit (Life Technologies), which is a membrane integrity assay. To quantify encapsulated cell viability, cell-laden hydrogels were incubated in AMVM culture media containing 1 mM calcein and 4 mM ethidium homodimer for 1 hour. For glass coverslips, cells were incubated in AMVM culture media containing 1 mM calcein and 4 mM ethidium homodimer for 30 minutes. Cells were imaged on widefield fluorescence microscope (EVOS M5000). To determine viability in 3D hydrogels, fraction of live cells was quantified by manual counting using live/dead staining. To calculate viability on glass coverslips, total-rod shaped cells were counted.

Immunofluorescence imaging

3D-encapsulated AMVMs were fixed with 4% paraformaldehyde (PFA) in PBS overnight at 4°C. The 3D hydrogels were then treated 24 h with blocking solution (TBS 0.05 M, pH 7.4, 10% FCS, 1% BSA, 0.5% Triton X-100) at 4°C. Overnight incubation of primary antibodies at 4°C was followed by 3x PBS washes (1 h each at room temperature). Primary antibody used were: monoclonal mouse anti α-actinin (1:1000; A7811 Sigma-Aldrich) rabbit anti-caveolin 3 (1:200; ab2912 Abcam) and mouse anti-YAP (1:1000; sc-101199) Santa Cruz Biotechnology) Secondary antibodies (goat anti-mouse Alexa Fluor 488 (1:500; Life Technologies), goat anti-rabbit Alexa Fluor 647 (1:500; Life Technologies)) and DAPI for nuclear staining were also incubated overnight at 4°C. 3x PBS washes (1 h each at room temperature) were performed before imaging.

AMVMs cultured on glass coverslips were fixed with 4% PFA in PBS for 30 minutes at 25°C. The AMVMs were permeabilized in 0.1% Triton X-100 for 6 minutes, and then treated 30 minutes with blocking solution (5% BSA in PBS) at 25°C. Overnight incubation of primary antibodies at 4°C was followed by 3x PBS washes (10 m each at room temperature). Secondary antibodies and DAPI for nuclear staining were also incubated 30 min at 25°C. 3x PBS washes (5 min at room temperature) were performed before imaging. Images were captured with a spinning disk confocal using either 20x or 40x air objectives (Nikon Ti-E).

Fast Fourier Transform (FFT) analysis

Analysis of α-actinin and caveolin-3 staining was performed using FFT analysis in ImageJ. The three central stacks for each cell were projected and a rectangular area of 8 × 50 μm was selected at the center of the cell and used for FFT. The signal of the Fourier order peak was fit using the following equation: $y = y0 + B * x + A * \exp\left(-2 * \left(\frac{x - x0}{W}\right)^2\right)$, where $y0$is the offset; B is the slope; A and W are amplitude and width of the peak of the FFT order and $x0$ is the center of the peak of the FFT order. Based on muscle diffraction theory (Judy et al., 1982), reduced amplitude or increased width of the peak of the FFT order is correlated to increase of the standard deviation of the periodic signal.

Cardiac myocyte contractility assay and analysis.

AMVMs encapsulated in 3D hydrogels onto 25mm coverslip were placed in a chamber system (IonOptix, Westwood, MA) provided with two platinum wires for electrical stimulation. The chamber was then transferred to the microscope (Nikon Diaphot) and superfused in Tyrode buffer (in mM): 113 NaCl, 4.7 KCl, 1.2 MgCl2, 10 glucose, and 10 HEPES; pH adjusted to 7.35 with NaOH. Myocytes were electrically paced via field stimulation at room temperature by using the IonOptix MyoPacer with a stimulus duration of 4ms, voltage of 1.2× stimulation threshold. Sarcomere shortening was recorded by IonWizard software (IonOptix, Westwood, MA). Representative trace was obtained by averaging ten consecutive contractions and analyzed. The following parameters were used: sarcomere shortening (%), time-to-peak of contractility (ms), relaxation time at 90% (ms). For comparison, AMVMs suspension was added onto a 25 mm coverslip and inserted in the

chamber system as described above, and allowed to settle for 5 minutes, prior to the beginning of contractility experiment.

Statistical analysis

Data are expressed and plotted as mean ± SEM (Standard Error of Mean) obtained from a number of independent determinations on different myocytes. Statistical numbers are indicated in the figure legends for each set of measurements. The statistical test used is reported in the figure legends. A p value of <0.05 is considered statistically significant (*$p < 0.05$,**$p < 0.01$, ***$p < 0.001$, ****$p < 0.0001$).

3. Results

Generation and characterization of PEG biocompatible hydrogels

PEG hydrogels formed by a thiol-ene click reaction were chosen based on proven cyto-compatibility and speed of polymerization (Fairbanks et al., 2009a). Hydrogels formulated with PEG norbornene (PEGnb) and PEG thiol (PEG-SH) were polymerized through a light-initiated step-growth polymerization, mediated by the photoinitiator lithium phenyl-2,4,6-trimethylbenzoylphosphinate (LAP) (Fig. 1A). The ligand CRGDS was added to promote cell adhesion, since α5β1 is one of the most highly expressed integrin heterodimers in cardiomyocytes and recognizes this sequence (Israeli-Rosenberg et al., 2014; Kapp et al., 2017). When exposed to low-intensity long-wave UV light, 2 mW/cm^2 of 365 nm light, hydrogels fully polymerized in < 20 seconds (Fig. 1B). We first aimed to develop a 3D hydrogel whose stiffness was similar to healthy adult mouse cardiac tissue. We measured the shear modulus of mouse left ventricles *ex vivo* using rheology. We found that mouse left ventricles are characterized by a shear modulus of ~4 kPa, and thus, we modulated the crosslinking density to generate hydrogels yielding a similar modulus (Fig. 1C). We then encapsulated AMVMs in 3D PEG hydrogels. Isolated AMVMs were mixed into the monomer solution. A drop of the cell-monomer suspension (30 μl) was added onto a coverslip where the shape was directed by a 6 mm diameter and 1 mm thick mold. The cell-monomer suspension was then exposed to light for 90 seconds to fully form the hydrogel (Fig. 1D). Cardiomyocytes plated onto glass coverslips coated with laminin were used as a control, as laminin coated glass coverslips represent the most used culture system for cardiomyocytes (Louch et al., 2011; O'Connell et al., 2007).

Cardiomyocyte viability in 3D hydrogels

To assess cell viability, we stained the 3D-encapsulated AMVMs with calcein and ethidium homodimer, a well-established membrane integrity assay. Cell viability was investigated at day 0 (after 3D encapsulation), days 1, 2, 3, and 5 (Fig. 2A). AMVMs cultured on glass coverslips were used as controls (Fig. 2B). At day 0, viable cardiomyocytes were at a density of 25-35 cells/mm^2 in both 3D PEG hydrogels and glass coverslips (~700-1000 cells per gel or glass coverslip). After 24 hours of culture (day 1) more than 50% (51.6 ± 15.6) of 3D encapsulated AMVMs were still viable compared to only 20% (19.9 ± 9.9) of cells cultured on glass coverslips. At day 2, the number of viable 3D-encapsulated cells was nearly halved (26.7 ± 9.6%), while less than 1% (0.6 ± 0.6) of viable cells was found on glass coverslips. At days 3 and 5 no viable cells were found on glass coverslips. In 3D

hydrogels, 8.8 ± 0.9% viable cells were found at day 3 but only 1.6 ± 1.6% at day 5 (Fig. 2C). The improved viability of AMVMs in 3D hydrogels as compared to glass coverslips indicates that a 3D culture system could represent a valuable tool to study mechanical cues in cardiac cells.

Cardiomyocyte cytoarchitecture in 3D hydrogels

As culturing cardiomyocytes has been associated with T-tubular remodeling and loss (Banyasz et al., 2008; Lipp et al., 1996; Mitcheson et al., 1996), we next investigated the architecture of T-tubules as well as sarcomeres of 2D cultured AMVMs on glass coverslips and 3D-encapsulated AMVMs cultured over time. Cells were stained with calcein before fixing in order to identify cells that were alive at the moment of collection. Calcein staining was maintained after the immunofluorescence staining protocol. Antibodies against α-actinin and caveolin-3 were used to label z-disks of sarcomere and T-tubules, respectively. By confocal imaging, only calcein-positive cells were selected to evaluate morphology of T-tubules and sarcomeres by immunofluorescence. 3D-encapsulated AMVMs showed well-organized sarcomeres and T-tubules at every time-point of culture (Fig. 3 A, C, D). In contrast, cells cultured on glass coverslips exhibited remodeled T-tubules at both days 1 and 2 of culture (Fig. 3B–D), and increased angular dispersion of sarcomere periodicity at day 2 of culture (Fig. 3B–C). Quantification of the T-tubule and sarcomere architecture by Fast-Fourier Transform (FFT) showed reduction of periodicity in cardiomyocytes cultured on glass-coverslips, as demonstrated by reduced amplitude and increased width of the FFT signal at day 2 of culture (Fig. 3C–D). In contrast, 3D-encapsulated AMVMs showed a progressive, but moderate, reduction of the periodic signals of both sarcomere and T-tubular architecture overtime (Fig. 3C–D).

Manipulation of hydrogels stiffness

Since tissue stiffness can change in different physiological and pathological settings, we encapsulated AMVMs in 3D hydrogels characterized by different shear moduli. In addition, the stiffness of PEG hydrogels can be increased dynamically after formation and cell encapsulation has occurred, by adding PEG monomers and LAP (Fig. S1A). We generated two more hydrogels with a shear modulus of 1.5, 4.7 kPa and 12.6 kPa, soft, medium, and stiff, respectively (Fig. 4A). We determined that AMVM viability was not dependent on the hydrogel stiffness, and thus, the material formulations could be tailored for 3D culture of AMVMs in microenvironments with a range of moduli to test their functional properties. Specifically, AMVMs encapsulated in the in soft, medium and stiff hydrogels did not show any statistically significant differences in viability after encapsulation (Fig. 4B), indicating that substrate crosslinking density did not affect cardiomyocyte viability. We also dynamically stiffened medium hydrogels to 12.6 kPa *in situ* (Fig. S1B) and AMVMs viability was not affected by the second exposure to light needed to increase the stiffness, as demonstrated by live/dead staining (Fig. S1C).

Cardiomyocyte contractility in 3D hydrogels

As a proof of principle that 3D hydrogel culture systems can be employed for functional studies, we performed contractility measurements of encapsulated AMVMs. Cell shortening was measured in AMVMs encapsulated in either soft, medium, or stiff 3D hydrogels 2 hours

post-encapsulation (day 0) (Fig. 4C). No difference in shortening, time to peak (TTP) and relaxation of contraction was found between AMVMs encapsulated in soft hydrogels as compared to cells on coverslips (Fig. 4D). However, AMVMs in stiff and medium hydrogels showed reduced shortening as compared to AMVMs on coverslips. Additionally, AMVMs in stiff hydrogels showed reduced shortening and increased relaxation as compared to AMVMs in soft hydrogels.

YAP translocation in response to hydrogel stiffness

Finally, we investigated the intracellular distribution of Yes-associated protein (YAP), a mechanosensitive transcriptional regulator, in AMVMs encapsulated in soft, medium, and stiff hydrogels compared to glass coverslips. YAP is a key mediator in mechanotransduction, and its translocation from the cytoplasm to the nucleus is associated with mechanical conditions that favor high intracellular forces (Halder et al., 2012). We immuno-stained AMVMs in 3D hydrogels and on glass coverslips for YAP and measured nuclear localization at days 0, 1, and 2 of culture (Fig. 5A; Table 1). After 2 hours post-encapsulation (day 0), we found that encapsulated AMVMs cultured in 3D hydrogels of varying stiffnesses showed differential YAP localization, measured by the ratio of nuclear to cytoplasmic intensity (N:C) (Fig. 5B). Medium and stiff hydrogels showed higher nuclear localization of YAP compared to soft hydrogels or glass coverslips (Fig. 5B). At day 1, we observed that AMVMs in medium stiffness hydrogels had reduced their N:C ratio, indicating active shuttling of YAP from the nucleus (Fig. 5C). On the other hand, the YAP N:C ratio remained elevated in AMVMs cultured in stiff hydrogels. By day 2, YAP N:C ratio decreased in AMVMs cultured in stiff hydrogels, and there were no significant differences in YAP N:C ratio between the soft, medium, and stiff hydrogels (Fig. 5D). AMVMs cultured on glass coverslips showed a decrease in YAP N:C over time, where at day 2 there was significantly reduced YAP N:C compared to AMVMs cultured in stiff hydrogels.

4. Discussion

The role of mechanical cues and mechanosensing in cell-matrix signaling is fundamentally important for a variety of cellular processes including migration (Hadden et al., 2017; Lo et al., 2000), development (Moore et al., 1995), cell fate determination (Engler et al., 2006), pathology (Georges et al., 2007; Zile et al., 2015) and death (Baines and Molkentin, 2005; Frisch and Francis, 1994). In adult cardiac tissue, the mechanical environment is highly dynamic and cardiac cells can adapt and respond to mechanical changes of the microenvironment in both physiological and pathological settings. *In vivo* studies are essential to delineate these phenomena in more relevant contexts, but do not allow for detailed dissection of the mechanisms involved. Cardiomyocyte cultures are commonly performed on tissue culture plastic or glass characterized by GPa-range stiffness, many orders of magnitude higher than physiological stiffness of the heart (Fig. 1C). Advances in biomaterial engineering have only recently allowed for assessment of cardiomyocyte responses in physiological (and pathological) extracellular stiffness (Galie et al., 2013; Ribeiro et al., 2015). Here, we demonstrate a 3D PEG-based hydrogel as a tool to finely control extracellular stiffness, extend survival, and investigate the effects of matrix

mechanical cues on isolated adult myocytes. To our knowledge, this is the first report of a 3D culture of adult rodent cardiomyocytes.

Previous work employing adult cardiomyocytes cultured on 2D polydimethylsiloxane (PDMS) with different stiffnesses has shown that myocytes can sense the mechanical properties of their microenvironment (Galie et al., 2013). The authors showed that substrate stiffness affects gene expression of structural proteins in cardiomyocytes, as well as contractility and calcium release over time. However, after 48 hours, the shape of cardiomyocytes in every culture condition appeared altered, and no comparison with the most common glass coverslip cultures was reported. In the present work, the well-preserved rod shape and the extended survival of AMVMs was maintained in our PEG culture. This might be due to the improved adhesion of cells to their microenvironment. In fact, in the context of a 3D culture system, cells can engage adhesion molecules present all around the cellular membrane and not only where one side of the cell, as on the coverslip or tissue culture plastic dish. 2D culture systems lack a physiologic microenvironment for cardiomyocytes, as the cells can only interact with the coverslip or substrate. In our work, mechanical load is distributed in three dimensions and could represent an interesting model to study Ca^{2+} release. Mechanical load is considered to have a pro-arrhythmogenic effect on hearts and cardiomyocytes in a relationship referred to as mechano-electric feedback (Kaufmann and Theophile, 1967). Previous studies using carbon fibers to acutely stretch isolated cardiomyocytes in one dimension have observed increased rates of Ca^{2+} sparks in stretched cells as compared to control (Iribe et al., 2009; Prosser et al., 2011). This is consistent with the presence of mechano-gated or mechanically-modulated ion channels on the cardiac sarcolemma and likely sarcoplasmic reticulum that can promote stretch-induced Ca^{2+} influx or release events (Jones et al., 2019; Peyronnet et al., 2016).

Our 3D culture system also demonstrated preserved T-tubular and sarcomere morphology of AMVMs after 72 hours of culture (Fig. 3). The maintenance of morphological features is quite promising, but it does not assess functional aspects of the T-tubules. In fact, structurally preserved T-tubules may not propagate action potentials (Crocini et al., 2014; Crocini et al., 2017; Crocini et al., 2016; Sacconi et al., 2012; Scardigli et al., 2017). Future studies should clarify whether our proposed PEG-based culture system also preserves function of T-tubules. Extended survival of adult cardiomyocytes could allow for improved studies employing viral infections or drug interventions. A window of 48-72 hours is typically used for efficient expression of a viral genome (O'Connell et al., 2007) and the preserved morphology of cardiomyocytes in the 3D culture could allow for improved localization studies, especially for T-tubular proteins. The time scale of the culture is still limited and might only be suitable to study acute drug effects. Efforts should be made towards extending cell viability. Different gel chemistries with a variety of functionalized groups could be tested for this type of culture. Additionally, cell culture medium could also be optimized, for instance a slightly more acidic culture environment (pH 6.9-7.0) could help improve maintenance of the rod shape of cardiomyocytes (Li et al., 2014).

We next demonstrated that AMVMs respond to stiffness when encapsulated in the 3D PEG hydrogels. AMVMs exhibited reduced shortening and increased nuclear localization of YAP with increased stiffness of the PEG hydrogel. We observed that our medium and stiff

hydrogels elicited more nuclear YAP accumulation than soft hydrogels, agreeing with the general consensus that YAP N:C increases with increasing substrate stiffness (Dupont et al., 2011). Interestingly, nuclear localization of YAP was low in AMVMs cultured on glass coverslips compared to 3D hydrogels. We posit this result may be due to the inability of the AMVMs to interact with or pull on the coverslips like they can in the hydrogels. Overall, these results suggest that AMVMs encapsulated in 3D PEG hydrogels actively respond to the mechanical cues offered by the microenvironment.

As PEG hydrogels have been extensively studied, there are many options for customizing the microenvironmental cues for studying specific cellular conditions, e.g. disease. The stiffness of our proposed PEG hydrogel can be dynamically increased through swelling of more PEG monomers (SI Fig. 1). Alternative PEG-based chemistries can instead been employed to reduce the environmental stiffness (Killaars et al., 2019). These features enable the possibility of studying dynamic cellular responses as a function of extracellular mechanical cues. Transitions from physiological to pathological stiffness and vice versa could be particularly useful to assess those cardiac pathologies characterized by increased fibrosis (Travers et al., 2016). For instance, increased left ventricular stiffness, as a result of excessive extracellular matrix, is a common trait in heart failure patients with preserved ejection fraction (Borlaug and Paulus, 2011). Numerous murine models for heart failure with preserved ejection fraction are available (Valero-Munoz et al., 2017) and could be potentially employed to assess shortening and relaxation at various stiffnesses.

Additionally, PEG hydrogels have been designed for tuning the biochemical environment both temporally and spatially with photolabile or photoreactive groups functionalized into the hydrogel itself (Kloxin et al., 2009). Through brief exposures to light, PEG hydrogels can release recombinant proteins to sustain cell growth, such as FGF-2 (Grim et al., 2015), or to provide specific biochemical cues.

In summary, we demonstrated that 3D PEG hydrogels extended AMVM viability, T-tubules and sarcomere integrity in culture and showed that AMVMs indeed respond to different stiffnesses. Continued work with 3D encapsulation of adult cells may be needed to improve culture times and viability to further understand how the microenvironment influences mature cardiac myocytes. This platform highlights how 3D culture of AMVMs may shed light into the progression and development of cardiac pathologies.

Supplementary Material

Refer to Web version on PubMed Central for supplementary material.

Acknowledgements:

We would like to acknowledge funding from the National Institutes of Health HL117138-05 and GM 029090-34 awarded to L.A.L; and R01 HL132353 awarded to K.A. C.C was supported by the Human Frontiers Science Program fellowship (LT001449/2017-L). C.J.W was supported by National Institutes of Health Predoctoral Fellowship F31HL142223. We would like to thank Tova Ceccato for providing PEG hydrogel monomers. Part of the imaging work was performed at the BioFrontiers Institute Advanced Light Microscopy Core directed by Dr. Joseph Dragavon.

References:

Baines CP and Molkentin JD, 2005 STRESS signaling pathways that modulate cardiac myocyte apoptosis, J Mol Cell Cardiol. 38, 47–62. [PubMed: 15623421]

Banyasz T, Lozinskiy I, Payne CE, Edelmann S, Norton B, Chen B, Chen-Izu Y, Izu LT and Balke CW, 2008 Transformation of adult rat cardiac myocytes in primary culture, Exp Physiol. 93, 370–82. [PubMed: 18156167]

Benton JA, Fairbanks BD and Anseth KS, 2009 Characterization of valvular interstitial cell function in three dimensional matrix metalloproteinase degradable PEG hydrogels, Biomaterials. 30, 6593–603. [PubMed: 19747725]

Borlaug BA and Paulus WJ, 2011 Heart failure with preserved ejection fraction: pathophysiology, diagnosis, and treatment, Eur Heart J. 32, 670–9. [PubMed: 21138935]

Brette F and Orchard C, 2003 T-tubule function in mammalian cardiac myocytes, Circ Res. 92, 1182–92. [PubMed: 12805236]

Chopra A, Lin V, McCollough A, Atzet S, Prestwich GD, Wechsler AS, Murray ME, Oake SA, Kresh JY and Janmey PA, 2012 Reprogramming cardiomyocyte mechanosensing by crosstalk between integrins and hyaluronic acid receptors, J Biomech. 45, 824–31. [PubMed: 22196970]

Crocini C, Coppini R, Ferrantini C, Yan P, Loew LM, Tesi C, Cerbai E, Poggesi C, Pavone FS and Sacconi L, 2014 Defects in T-tubular electrical activity underlie local alterations of calcium release in heart failure, Proc Natl Acad Sci U S A. 111, 15196–201. [PubMed: 25288764]

Crocini C, Ferrantini C, Coppini R and Sacconi L, 2017 Electrical defects of the transverse-axial tubular system in cardiac diseases, J Physiol. 595, 3815–3822. [PubMed: 27981580]

Crocini C, Ferrantini C, Scardigli M, Coppini R, Mazzoni L, Lazzeri E, Pioner JM, Scellini B, Guo A, Song LS, Yan P, Loew LM, Tardiff J, Tesi C, Vanzi F, Cerbai E, Pavone FS, Sacconi L and Poggesi C, 2016 Novel insights on the relationship between T-tubular defects and contractile dysfunction in a mouse model of hypertrophic cardiomyopathy, J Mol Cell Cardiol. 91, 42–51. [PubMed: 26714042]

Dupont S, Morsut L, Aragona M, Enzo E, Giulitti S, Cordenonsi M, Zanconato F, Le Digabel J, Forcato M, Bicciato S, Elvassore N and Piccolo S, 2011 Role of YAP/TAZ in mechanotransduction, Nature. 474, 179–83. [PubMed: 21654799]

Engler AJ, Sen S, Sweeney HL and Discher DE, 2006 Matrix elasticity directs stem cell lineage specification, Cell. 126, 677–89. [PubMed: 16923388]

Fairbanks BD, Schwartz MP, Bowman CN and Anseth KS, 2009a Photoinitiated polymerization of PEG-diacrylate with lithium phenyl-2,4,6-trimethylbenzoylphosphinate: polymerization rate and cytocompatibility, Biomaterials. 30, 6702–7. [PubMed: 19783300]

Fairbanks BD, Schwartz MP, Halevi AE, Nuttelman CR, Bowman CN and Anseth KS, 2009b A Versatile Synthetic Extracellular Matrix Mimic via Thiol-Norbornene Photopolymerization, Adv Mater. 21, 5005–5010. [PubMed: 25377720]

Ferrantini C, Crocini C, Coppini R, Vanzi F, Tesi C, Cerbai E, Poggesi C, Pavone FS and Sacconi L, 2013 The transverse-axial tubular system of cardiomyocytes, Cell Mol Life Sci. 70, 4695–710. [PubMed: 23846763]

Frisch SM and Francis H, 1994 Disruption of epithelial cell-matrix interactions induces apoptosis, J Cell Biol. 124, 619–26. [PubMed: 8106557]

Galie PA, Khalid N, Carnahan KE, Westfall MV and Stegemann JP, 2013 Substrate stiffness affects sarcomere and costamere structure and electrophysiological function of isolated adult cardiomyocytes, Cardiovasc Pathol. 22, 219–27. [PubMed: 23266222]

Georges PC, Hui JJ, Gombos Z, McCormick ME, Wang AY, Uemura M, Mick R, Janmey PA, Furth EE and Wells RG, 2007 Increased stiffness of the rat liver precedes matrix deposition: implications for fibrosis, Am J Physiol Gastrointest Liver Physiol. 293, G1147–54. [PubMed: 17932231]

Gourdie RG, Dimmeler S and Kohl P, 2016 Novel therapeutic strategies targeting fibroblasts and fibrosis in heart disease, Nat Rev Drug Discov. 15, 620–38. [PubMed: 27339799]

Grim JC, Marozas IA and Anseth KS, 2015 Thiol-ene and photo-cleavage chemistry for controlled presentation of biomolecules in hydrogels, J Control Release. 219, 95–106. [PubMed: 26315818]

Hadden WJ, Young JL, Holle AW, McFetridge ML, Kim DY, Wijesinghe P, Taylor-Weiner H, Wen JH, Lee AR, Bieback K, Vo BN, Sampson DD, Kennedy BF, Spatz JP, Engler AJ and Choi YS, 2017 Stem cell migration and mechanotransduction on linear stiffness gradient hydrogels, Proc Natl Acad Sci U S A. 114, 5647–5652. [PubMed: 28507138]

Halder G, Dupont S and Piccolo S, 2012 Transduction of mechanical and cytoskeletal cues by YAP and TAZ, Nat Rev Mol Cell Biol. 13, 591–600. [PubMed: 22895435]

Hazeltine LB, Simmons CS, Salick MR, Lian X, Badur MG, Han W, Delgado SM, Wakatsuki T, Crone WC, Pruitt BL and Palecek SP, 2012 Effects of substrate mechanics on contractility of cardiomyocytes generated from human pluripotent stem cells, Int J Cell Biol. 2012, 508294. [PubMed: 22649451]

Hirt MN, Boeddinghaus J, Mitchell A, Schaaf S, Bornchen C, Muller C, Schulz H, Hubner N, Stenzig J, Stoehr A, Neuber C, Eder A, Luther PK, Hansen A and Eschenhagen T, 2014 Functional improvement and maturation of rat and human engineered heart tissue by chronic electrical stimulation, J Mol Cell Cardiol. 74, 151–61. [PubMed: 24852842]

Iribe G, Ward CW, Camelliti P, Bollensdorff C, Mason F, Burton RA, Garny A, Morphew MK, Hoenger A, Lederer WJ and Kohl P, 2009 Axial stretch of rat single ventricular cardiomyocytes causes an acute and transient increase in Ca2+ spark rate, Circ Res. 104, 787–95. [PubMed: 19197074]

Israeli-Rosenberg S, Manso AM, Okada H and Ross RS, 2014 Integrins and integrin-associated proteins in the cardiac myocyte, Circ Res. 114, 572–586. [PubMed: 24481847]

Jones JL, Peana D, Veteto AB, Lambert MD, Nourian Z, Karasseva NG, Hill MA, Lindman BR, Baines CP, Krenz M and Domeier TL, 2019 TRPV4 increases cardiomyocyte calcium cycling and contractility yet contributes to damage in the aged heart following hypoosmotic stress, Cardiovasc Res. 115, 46–56. [PubMed: 29931225]

Judy MM, Summerour V, LeConey T, Roa RL and Templeton GH, 1982 Muscle diffraction theory. Relationship between diffraction subpeaks and discrete sarcomere length distributions, Biophys J. 37, 475–87. [PubMed: 7059651]

Kapp TG, Rechenmacher F, Neubauer S, Maltsev OV, Cavalcanti-Adam EA, Zarka R, Reuning U, Notni J, Wester HJ, Mas-Moruno C, Spatz J, Geiger B and Kessler H, 2017 A Comprehensive Evaluation of the Activity and Selectivity Profile of Ligands for RGD-binding Integrins, Sci Rep. 7, 39805. [PubMed: 28074920]

Kaufmann R and Theophile U, 1967 [Autonomously promoted extension effect in Purkinje fibers, papillary muscles and trabeculae carneae of rhesus monkeys], Pflugers Arch Gesamte Physiol Menschen Tiere. 297, 174–89.

Killaars AR, Grim JC, Walker CJ, Hushka EA, Brown TE and Anseth KS, 2019 Extended Exposure to Stiff Microenvironments Leads to Persistent Chromatin Remodeling in Human Mesenchymal Stem Cells, Adv Sci (Weinh). 6, 1801483. [PubMed: 30775233]

Kloxin AM, Kasko AM, Salinas CN and Anseth KS, 2009 Photodegradable hydrogels for dynamic tuning of physical and chemical properties, Science. 324, 59–63. [PubMed: 19342581]

Kong P, Christia P and Frangogiannis NG, 2014 The pathogenesis of cardiac fibrosis, Cell Mol Life Sci. 71, 549–74. [PubMed: 23649149]

Leijten J, Seo J, Yue K, Santiago GT, Tamayol A, Ruiz-Esparza GU, Shin SR, Sharifi R, Noshadi I, Alvarez MM, Zhang YS and Khademhosseini A, 2017 Spatially and Temporally Controlled Hydrogels for Tissue Engineering, Mater Sci Eng R Rep. 119, 1–35. [PubMed: 29200661]

Li D, Wu J, Bai Y, Zhao X and Liu L, 2014 Isolation and culture of adult mouse cardiomyocytes for cell signaling and in vitro cardiac hypertrophy, J Vis Exp.

Lin CC and Anseth KS, 2009 PEG hydrogels for the controlled release of biomolecules in regenerative medicine, Pharm Res. 26, 631–43. [PubMed: 19089601]

Lipp P, Huser J, Pott L and Niggli E, 1996 Spatially non-uniform Ca2+ signals induced by the reduction of transverse tubules in citrate-loaded guinea-pig ventricular myocytes in culture, J Physiol. 497 (Pt 3), 589–97. [PubMed: 9003546]

Lo CM, Wang HB, Dembo M and Wang YL, 2000 Cell movement is guided by the rigidity of the substrate, Biophys J. 79, 144–52. [PubMed: 10866943]

Louch WE, Sheehan KA and Wolska BM, 2011 Methods in cardiomyocyte isolation, culture, and gene transfer, J Mol Cell Cardiol. 51, 288–98. [PubMed: 21723873]

Mabry KM, Lawrence RL and Anseth KS, 2015 Dynamic stiffening of poly(ethylene glycol)-based hydrogels to direct valvular interstitial cell phenotype in a three-dimensional environment, Biomaterials. 49, 47–56. [PubMed: 25725554]

Mitcheson JS, Hancox JC and Levi AJ, 1996 Action potentials, ion channel currents and transverse tubule density in adult rabbit ventricular myocytes maintained for 6 days in cell culture, Pflugers Arch. 431, 814–27. [PubMed: 8927497]

Moore SW, Keller RE and Koehl MA, 1995 The dorsal involuting marginal zone stiffens anisotropically during its convergent extension in the gastrula of Xenopus laevis, Development. 121, 3131–40. [PubMed: 7588048]

O'Connell TD, Rodrigo MC and Simpson PC, 2007 Isolation and culture of adult mouse cardiac myocytes, Methods Mol Biol. 357, 271–96. [PubMed: 17172694]

Peyronnet R, Nerbonne JM and Kohl P, 2016 Cardiac Mechano-Gated Ion Channels and Arrhythmias, Circ Res. 118, 311–29. [PubMed: 26838316]

Porter KE and Turner NA, 2009 Cardiac fibroblasts: at the heart of myocardial remodeling, Pharmacol Ther. 123, 255–78. [PubMed: 19460403]

Prosser BL, Ward CW and Lederer WJ, 2011 X-ROS signaling: rapid mechano-chemo transduction in heart, Science. 333, 1440–5. [PubMed: 21903813]

Ribeiro AJ, Ang YS, Fu JD, Rivas RN, Mohamed TM, Higgs GC, Srivastava D and Pruitt BL, 2015 Contractility of single cardiomyocytes differentiated from pluripotent stem cells depends on physiological shape and substrate stiffness, Proc Natl Acad Sci U S A. 112, 12705–10. [PubMed: 26417073]

Rodriguez AG, Schroeder ME, Walker CJ and Anseth KS, 2018 FGF-2 inhibits contractile properties of valvular interstitial cell myofibroblasts encapsulated in 3D MMP-degradable hydrogels, APL Bioengineering. 2, 046104. [PubMed: 31069326]

Ronaldson-Bouchard K, Ma SP, Yeager K, Chen T, Song L, Sirabella D, Morikawa K, Teles D, Yazawa M and Vunjak-Novakovic G, 2018 Advanced maturation of human cardiac tissue grown from pluripotent stem cells, Nature. 556, 239–243. [PubMed: 29618819]

Ruan JL, Tulloch NL, Razumova MV, Saiget M, Muskheli V, Pabon L, Reinecke H, Regnier M and Murry CE, 2016 Mechanical Stress Conditioning and Electrical Stimulation Promote Contractility and Force Maturation of Induced Pluripotent Stem Cell-Derived Human Cardiac Tissue, Circulation. 134, 1557–1567. [PubMed: 27737958]

Sacconi L, Ferrantini C, Lotti J, Coppini R, Yan P, Loew LM, Tesi C, Cerbai E, Poggesi C and Pavone FS, 2012 Action potential propagation in transverse-axial tubular system is impaired in heart failure, Proc Natl Acad Sci U S A. 109, 5815–9. [PubMed: 22451916]

Scardigli M, Crocini C, Ferrantini C, Gabbrielli T, Silvestri L, Coppini R, Tesi C, Rog-Zielinska EA, Kohl P, Cerbai E, Poggesi C, Pavone FS and Sacconi L, 2017 Quantitative assessment of passive electrical properties of the cardiac T-tubular system by FRAP microscopy, Proc Natl Acad Sci U S A. 114, 5737–5742. [PubMed: 28507142]

Schultz KM, Kyburz KA and Anseth KS, 2015 Measuring dynamic cell-material interactions and remodeling during 3D human mesenchymal stem cell migration in hydrogels, Proc Natl Acad Sci U S A. 112, E3757–64. [PubMed: 26150508]

Tibbitt MW and Anseth KS, 2009 Hydrogels as extracellular matrix mimics for 3D cell culture, Biotechnol Bioeng. 103, 655–63. [PubMed: 19472329]

Travers JG, Kamal FA, Robbins J, Yutzey KE and Blaxall BC, 2016 Cardiac Fibrosis: The Fibroblast Awakens, Circ Res. 118, 1021–40. [PubMed: 26987915]

Valero-Munoz M, Backman W and Sam F, 2017 Murine Models of Heart Failure with Preserved Ejection Fraction: a "Fishing Expedition", JACC Basic Transl Sci. 2, 770–789. [PubMed: 29333506]

Zile MR, Baicu CF, Ikonomidis JS, Stroud RE, Nietert PJ, Bradshaw AD, Slater R, Palmer BM, Van Buren P, Meyer M, Redfield MM, Bull DA, Granzier HL and LeWinter MM, 2015 Myocardial stiffness in patients with heart failure and a preserved ejection fraction: contributions of collagen and titin, Circulation. 131, 1247–59. [PubMed: 25637629]

Zustiak SP and Leach JB, 2010 Hydrolytically degradable poly(ethylene glycol) hydrogel scaffolds with tunable degradation and mechanical properties, Biomacromolecules. 11, 1348–57. [PubMed: 20355705]

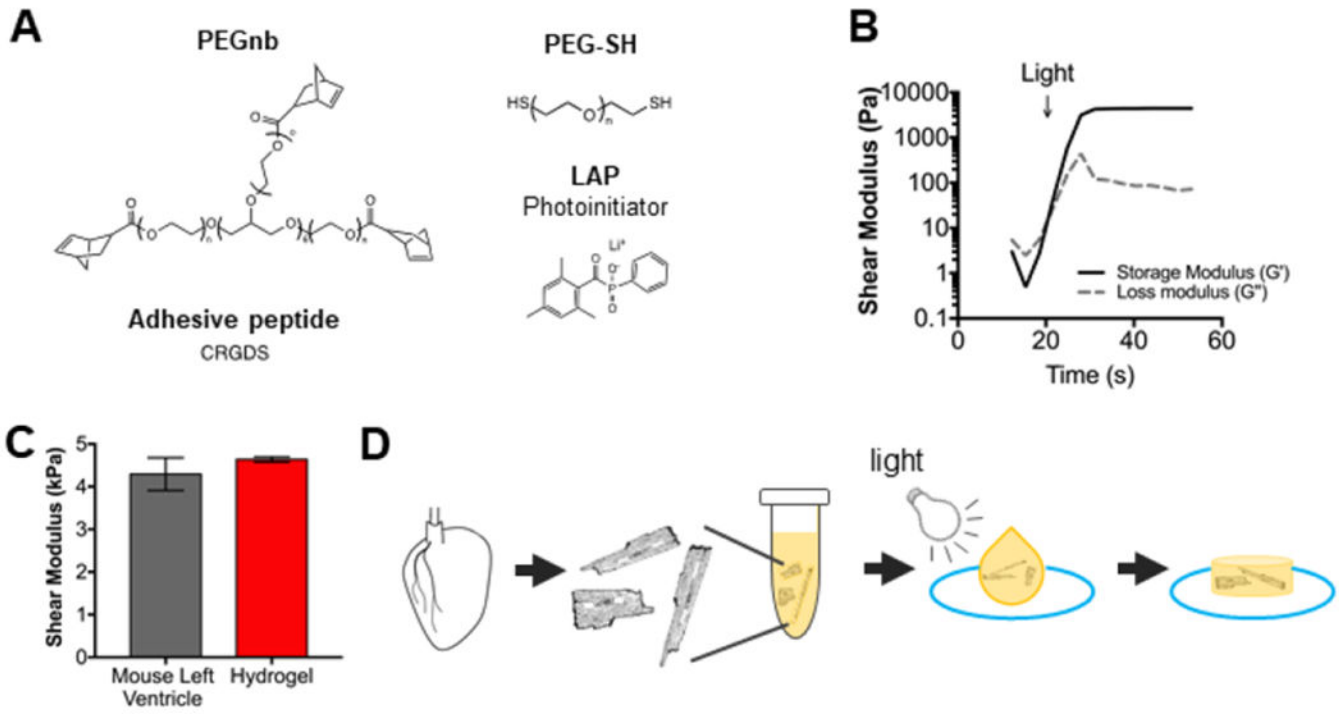

Figure 1: Thiol-ene PEG hydrogels for adult mouse cardiac myocytes 3D encapsulation and culture.

A) Hydrogel matrices were formed by a photoinitiated thiol-ene polymerization of 8-arm poly(ethylene glycol) (PEGnb) (40 kDa) and poly(ethylene glycol) dithiol (PEG-SH). An adhesive peptide, CRGDS, was incorporated to facilitate cell adhesion to the hydrogels. B) Average rheological trace of hydrogel gelation in response to light, n=4. Hydrogel light-initiated polymerization was measured by shear rheology. At indicated time, light was turned on for 90 sec at 365 nm; 2 mW cm-2. Hydrogel gelation point is indicated by the crossover of the storage and loss modulus. C) The shear modulus for healthy adult mouse left ventricle and PEG hydrogels. Shear modulus was measured by shear rheology. n=11 mice, n=9 hydrogels. Data reported as mean ± SEM. D) Schematic of 3D encapsulation of adult mouse cardiac myocytes (AMVMs) in PEG hydrogels. Isolated AMVMs were mixed with hydrogel monomers, placed into cylindrical molds, polymerized with light for 90 sec, and placed into appropriate media.

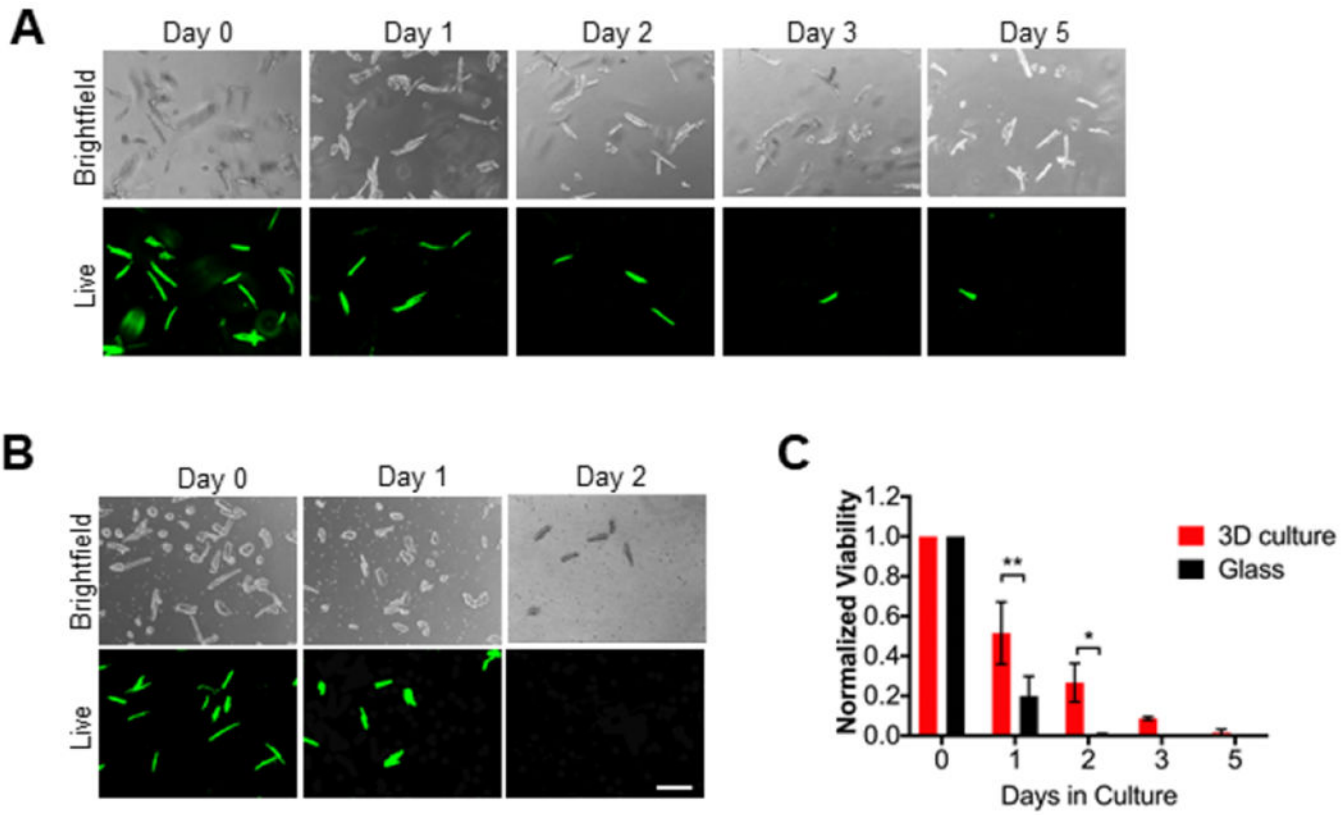

Figure 2: Adult mouse cardiomyocytes can be cultured in 3D PEG hydrogels for extended times.

A) Representative brightfield and live images of adult mouse cardiac myocytes (AMVMs) cultured in 3D PEG hydrogels for 0, 1, 2, 3, or 5 days. Cells were cultured with calcein (Live) and ethidium homodimer for 1 hour prior to imaging. Scale bar = 200um. B) Representative brightfield and live images of AMVMs cultured on glass coverslips for 0, 1, 2 days. Cells were cultured with calcein and ethidium homodimer for 30 minutes prior to imaging. Scale bar = 200 um. C) Quantification of AMVM viability in 3D culture and glass coverlsips over 0, 1, 2, 3, or 5 days. For 3D culture N=3 mice, for glass N=4 mice. Two-way ANOVA with Bonferroni post-hoc test applied; *p<0.5 **p < 0.01. Data reported as mean ± SEM.

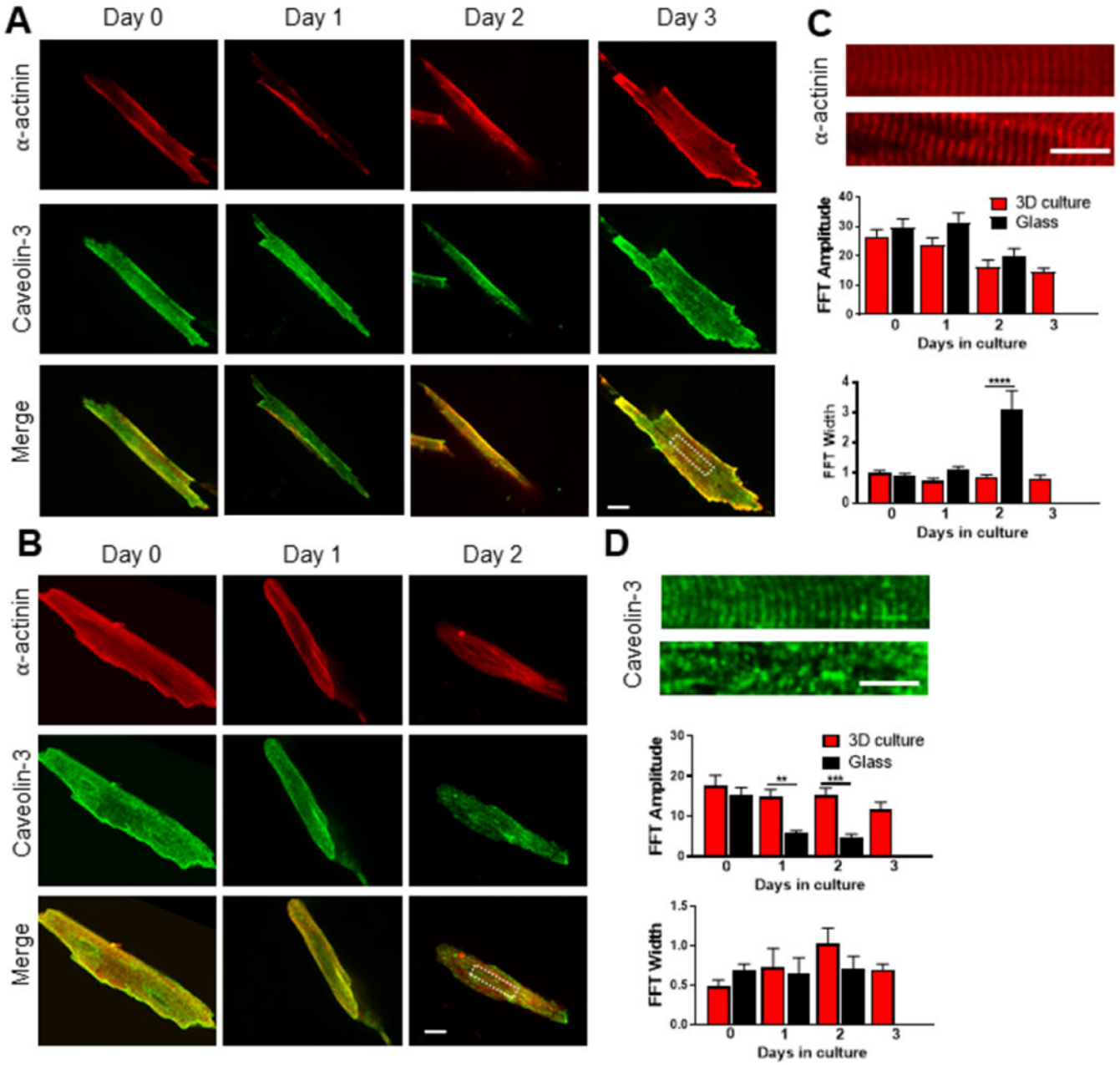

Figure 3: Sarcomeric structure and t-tubules are preserved in adult mouse cardiomyocytes cultured in 3D PEG hydrogels over time.

A) Representative immunofluorescence images of 3D-cultured adult mouse cardiomyocytes stained for α-actinin (red) and caveolin-3 (green) over time. Viability of cells at the moment of fixing was evaluated by calcein staining, which is retained after the staining protocol. Merge image at the bottom of the panel. Scale bar = 20 μm in white. B) Representative images of adult mouse cardiomyocytes cultured on glass coverslips stained for α-actinin (red) and caveolin-3 (green) over time. Merge image at the bottom of the panel. Scale bar = 20 μm in white. C) Above, magnification of the red channel from the white insets reported in panel A and B, respectively. Scale bar = 10 μm in white. Below, column graphs reporting the

amplitude and width of the fast Fourier order. n=5 per group. D) Above, magnification of the green channel from the white insets reported in panel A and B, respectively. Scale bar = 10 μm in white. Below, column graphs reporting the amplitude and width of the fast Fourier order. n=5 per group. One-way ANOVA with Bonferroni post-hoc test applied; **p<0.01; ***p<0.0001; ****p < 0.00001. Data reported as mean ± SEM.

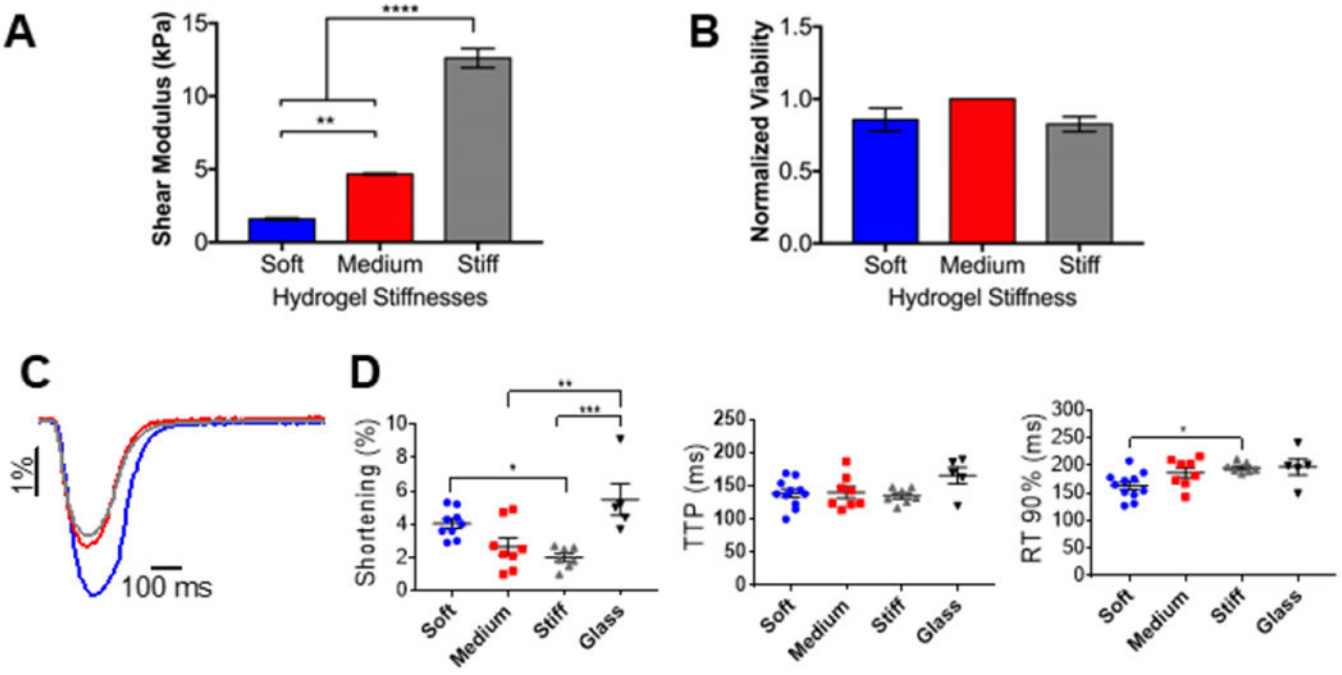

Figure 4: Adult mouse cardiomyocytes contractility is affected by different stiffnesses.

A) Columns showing the shear modulus for different thiol-ene PEG hydrogels, measured by shear rheology. Data reported as mean ± SEM. One-way ANOVA with Bonferroni post-hoc test applied; **p < 0.01, ****p < 0.0001. B) Viability of adult mouse cardiomyocytes encapsulated in thiol-ene PEG hydrogels with different stiffnesses at day 0 (2 hours post-encapsulation). Viability assessed by calcein/ethidium homodimer staining and reported as % normalized to cells encapsulated in medium stiffness PEG hydrogel. Data reported as mean ± SEM, N=3. C) Representative cell shortening traces of adult mouse cardiomyocytes encapsulated in soft, medium, or stiff PEG hydrogels (blue, red, and grey, respectively). D) Graphs showing shortening, time-to-peak (TTP) and relaxation 90% (RT90%) of adult mouse cardiomyocytes encapsulated in soft, medium, stiff PEG hydrogels, or not encapsulated. Data reported as scatter plots with the central line representing the mean value, and the error bars representing SEM from n=10 cells (soft), n=8 cells (medium), n=7 cells (stiff), and n=5 cells (no gel). N=3 (number of animals). One-way ANOVA with Bonferroni post-hoc test applied; *p<0.5 **p < 0.01, ***p < 0.001.

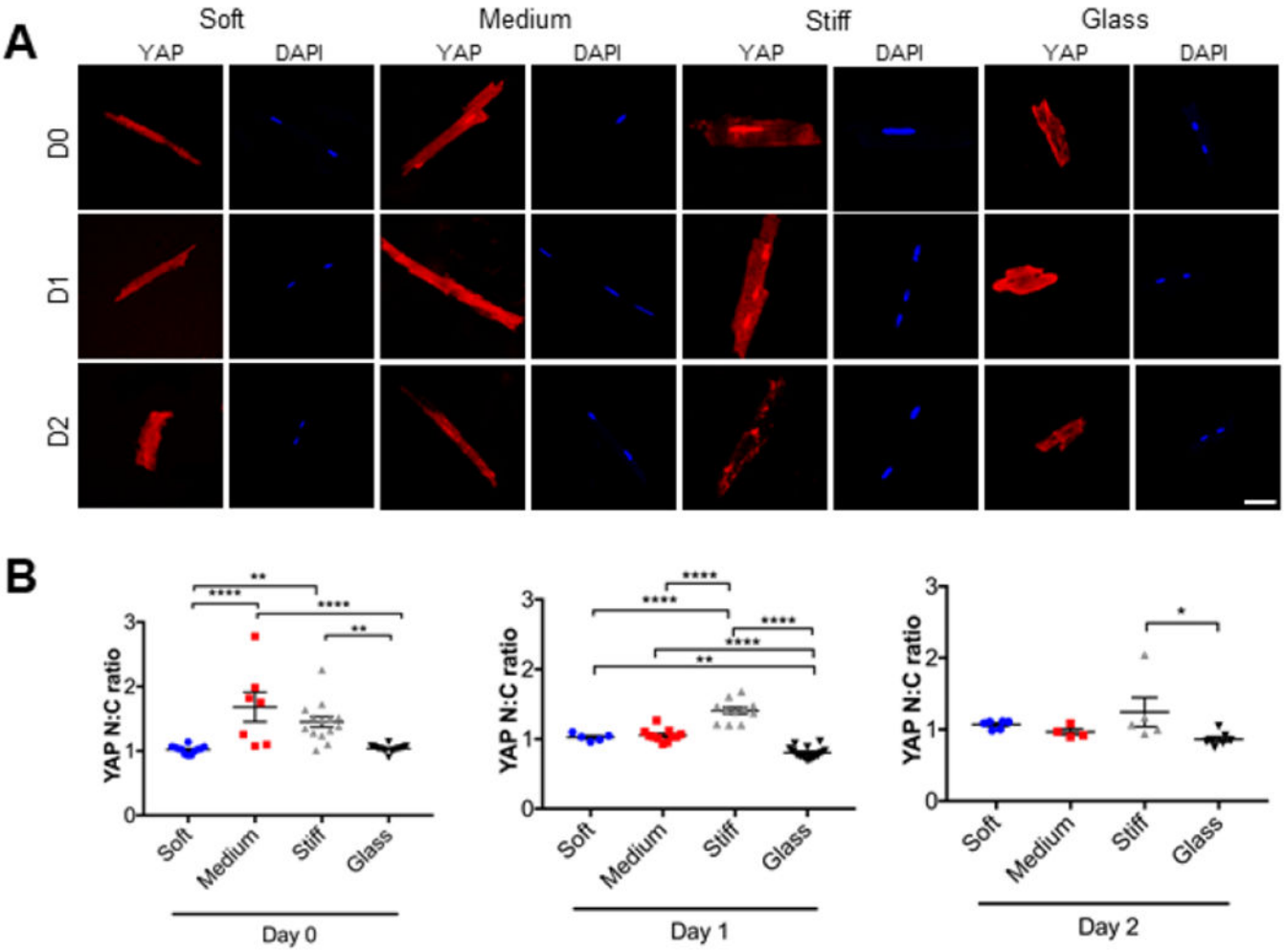

Figure 5: YAP translocation in adult mouse cardiomyocytes responds differently to various stiffnesses over time.

A) Representative immunofluorescence images of adult mouse cardiomyocytes stained for YAP (red). Nuclear staining is DAPI (blue). Cells were cultured in soft, medium, or stiff 3D PEG hydrogels or onto glass coverslips over time. B) Graphs showing the ratio between nuclear and cytoplasmic localization of YAP. Nuclei detected with DAPI. Data reported as scatter plot with the central line representing the mean value, and the error bars representing SEM from day 0: n=12 nuclei (soft), n=7 nuclei (medium), n=14 nuclei (stiff), and n=14 nuclei (glass); day 1: n=5 nuclei (soft), n=11 nuclei (medium), n=11 nuclei (stiff), and n=14 nuclei (glass). day 2: n=6 nuclei (soft), n=4 nuclei (medium), n=5 nuclei (stiff), and n=7 nuclei (glass). N=2 (number of animals). One-way ANOVA with Bonferroni post-hoc test applied; *p<0.5, **p<0.01, ***p < 0.001, ****p<0.0001.

Table 1.

YAP N:C ratio in AMVMs cultured in 3D PEG hydrogels and glass coverslips overtime.

	Soft			Medium			Stiff			Glass		
DAYS	**0**	**1**	**2**	**0**	**1**	**2**	**0**	**1**	**2**	**0**	**1**	**2**
	1.067	1.099	1.003	1.820	1.120	0.896	1.008	1.477	1.165	0.997	0.733	0.830
	1.057	0.992	1.114	1.077	1.047	1.085	1.317	1.469	0.998	1.044	0.706	0.749
	1.064	1.047	0.986	1.257	0.951	0.919	1.236	1.413	2.044	1.057	0.800	0.852
	1.138	0.959	1.087	1.100	1.009	0.968	1.101	1.204	0.942	1.015	0.936	0.914
	1.034	1.032	1.108	2.778	1.068		1.279	1.212	1.066	1.003	0.966	1.045
	1.026		1.108	1.985	0.929		1.348	1.202		0.901	0.831	0.850
	0.999			1.754	1.031		1.384	1.375		1.022	0.745	0.808
	0.930				1.031		1.506	1.428		1.030	0.861	
	1.036				1.105		1.638	1.681		1.068	0.736	
	0.950				1.265		1.485	1.606		1.040	0.689	
	1.027				1.028		1.517	1.392		1.037	0.886	
	0.933						1.520			1.074	0.759	
							2.259			1.076	0.825	
							1.723			1.142	0.770	